Sains Malaysiana 46(9)(2017): 1667–1674
http://dx.doi.org/10.17576/jsm-2017-4609-40

Unsteady Flow of a Nanofluid Past a Permeable Shrinking Cylinder using Buongiorno's Model

(Aliran Tak Mantap Nanobendalir melalui Silinder Telap Mengecut menggunakan model Buongiorno)

KHAIRY ZAIMI*, ANUAR ISHAK & IOAN POP

ABSTRACT

The unsteady laminar boundary layer flow of a nanofluid and heat transfer over a permeable shrinking cylinder using the Buongiorno's nanofluid model is investigated. Using a similarity transformation, the governing partial differential equations are transformed into a system of ordinary differential equations and then solved numerically using a shooting method. The numerical results are obtained for velocity, temperature and concentration profiles as well as the skin friction coefficient, the local Nusselt number and the local Sherwood number. Dual solutions are found to exist in a certain range of the suction and unsteadiness parameters. It is observed that suction parameter increase both the skin friction coefficient and the heat transfer rate at the surface, whereas the opposite trend is obtained for the Sherwood number. It is also observed that suction widens the range of the unsteadiness parameter for which the solution exists.

Keywords: Nanofluids; shrinking cylinder; suction; unsteady flow

ABSTRAK

Aliran lapisan sempadan lamina tak mantap nanobendalir dan pemindahan haba terhadap silinder telap mengecut menggunakan model nanobendalir Buongiorno dikaji. Menggunakan penjelmaan keserupaan, persamaan menakluk dalam bentuk persamaan pembezaan separa dijelmakan kepada persamaan pembezaan biasa dan diselesaikan secara berangka menggunakan kaedah tembakan. Keputusan berangka diperoleh bagi profil-profil halaju, suhu dan pecahan isi padu nanozarah serta pekali geseran kulit, nombor Nusselt setempat dan nombor Sherwood setempat. Penyelesaian dual didapati wujud bagi julat-julat tertentu parameter sedutan dan parameter ketakmantapan. Didapati parameter sedutan meningkatkan pekali geseran kulit dan kadar pemindahan haba pada permukaan, manakala telatah bertentangan diperoleh bagi nombor Sherwood. Didapati juga sedutan meluaskan julat parameter ketakmantapan yang penyelesaian wujud.

Kata kunci: Aliran tak mantap; nanobendalir; sedutan; silinder mengecut

INTRODUCTION

The flow and heat transfer due to a stretching/shrinking sheet has become an important problem in engineering processes with application in industries such as in metal, food and plastic productions (Wang 1988). It has gained considerable interest among large number of researchers since the past few decades. Recently, a quite number of studies have been carried out on stretching/shrinking cylinder. The pioneering work on this topic was done by Wang (1988) when investigating the flow outside a stretching hollow cylinder in an ambient fluid. This problem was then extended by Ishak et al. (2008a, 2008b) with uniform suction/injection and magnetic field effects. Later, Wang and Ng (2011) obtained the similarity solution due to a stretching of a cylinder with a partial slip boundary condition, while Wang (2012) investigated the flow and mixed convection due to a vertical stretching cylinder. The flow over an expanding stretching cylinder was analyzed by Fang et al. (2011). In a subsequent paper, Fang et al. (2012) updated the latest development in this topic by solving the unsteady viscous flow on the outside of an expanding or contracting cylinder. Mukhopadhyay (2012) studied a steady mixed convection boundary layer flow and heat transfer over a stretching cylinder in a porous medium and found the similarity solutions using the shooting method. Recently, Wan Zaimi et al. (2013) have solved numerically the unsteady viscous flow due to a shrinking cylinder with suction effect using a shooting method. The duality nature of the solution was reported for a certain range of the suction and unsteadiness parameters. On the other hand, Dhanai et al. (2016) investigated numerically the mixed convection flow and heat transfer of uniformly conducting nanofluid over an inclined cylinder using the Buongiorno's nanofluid model under the influence of slip and viscous dissipation effects. Most recently, Mohamed et al. (2016) investigated the effect of viscous dissipation on the free convection boundary layer flow over a horizontal circular cylinder in a nanofluid with constant wall temperature.

There are some applications on the flow over a stretching/shrinking cylinder in industrial and engineering processes. Simal et al. (1998) developed a sample shrinkage model, which is useful for the simulation of the drying curves of broccoli stems at different air drying temperatures and sample lengths, thus can predict the drying times and end-point of a drying process. They also insisted that their model could be applied to simulate the drying curves of different biological and cylindrical products.

The considerable interest received for the flow in a nanofluid is motivated by the fact that nanofluids provide good stability and rheological properties (Duangthongsuk & Wongwises 2008). The term ‘nanofluid’, defined as a mixture of nanoparticles and the base fluid e.g. water and oil was first coined by Choi (1995). This mixture is able to enhance the thermal conductivity and convective heat transfer coefficient compared to the base fluid (Kakac & Pramuanjaroenkij 2009). A good literature review on this topic can be found in the book by Das et al. (2007) and in the review papers by Buongiorno (2006), Duangthongsuk and Wongwises (2008), Kakac and Pramuanjaroenkij (2009), Trisaksri and Wongwises (2007) and Wang and Mujumdar (2008).

The aim of the present paper was to investigate the unsteady flow due to a permeable shrinking cylinder in a nanofluid using the model proposed by Buongiorno (2006). In this work, we focus on the flow induced by a shrinking cylinder in a nanofluid that particularly has not been considered before. This study also concern on the flow over a shrinking cylinder with a time-dependent diameter and the flow is control by the unsteadiness parameter. The present problem is formulated in such a manner that the partial differential equations governing the flow, temperature and concentration fields are first transformed to ordinary differential equations, which are solved numerically using a shooting method. To understand the flow behavior and heat transfer characteristics, results are obtained for the skin friction coefficient, the Nusselt number and the Sherwood number which are presented graphically and discussed.

Mathematical Formulation

Consider an unsteady laminar boundary layer flow of a nanofluid over a circular cylinder in shrinking motion as shown in Figure 1. It is assumed that the diameter of the cylinder is a function of time with unsteady radius $a(t) = a_0\sqrt{1-\beta t}$, where β is the constant of the expansion/contraction strength, t is the time and a_0 is the radius of the cylinder at the initial time $t = 0$. For the unsteady and incompressible nanofluids, the following four equations embodying the conservation of mass, momentum, thermal energy and nanoparticle volume fraction in the vectorial form are (Buongiorno 2006; Kuznetsov & Nield 2010),

Continuity:

$$\nabla \cdot \mathbf{v} = 0. \tag{1}$$

Momentum:

$$\frac{\partial \mathbf{v}}{\partial t} + \mathbf{v}\cdot\nabla\mathbf{v} = -\frac{1}{\rho}\nabla p + \nu\,\nabla^2\mathbf{v}. \tag{2}$$

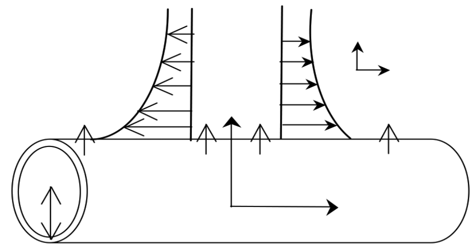

FIGURE 1. A schematic model and coordinate system

Thermal energy:

$$\frac{\partial T}{\partial t} + \mathbf{v}\cdot\nabla T = \alpha\nabla^2 T + \tau\left[D_B\nabla T\cdot\nabla C + (D_T/T_\infty)\nabla T\cdot\nabla T\right]. \tag{3}$$

Nanoparticle volume fraction:

$$\frac{\partial C}{\partial t} + \mathbf{v}\cdot\nabla C = D_B\nabla^2 C + \left(D_T/T_\infty\right)\nabla^2 T \tag{4}$$

where $\mathbf{v} = \langle u, w\rangle$ is the velocity vector; T is the temperature C is the nanoparticle volume fraction; p is the pressure; ν is the kinematic viscosity; ρ is the fluid density; D_B is the Brownian diffusion coefficient; and D_T is the thermophoretic diffusion coefficient.

Based on the axisymmetric flow assumptions and that there is no azimuthal velocity component, the three-dimensional unsteady Navier-Stokes equations for incompressible fluid without body force in cylindrical coordinates, (1) - (4) can be written as (Bejan 2013).

Continuity:

$$\frac{1}{r}\frac{\partial}{\partial r}(ru) + \frac{\partial w}{\partial z} = 0. \tag{5}$$

Momentum:

$$\frac{\partial u}{\partial t} + u\frac{\partial u}{\partial r} + w\frac{\partial u}{\partial z} = -\frac{1}{\rho}\frac{\partial p}{\partial r} + \nu\left(\frac{\partial^2 u}{\partial r^2} + \frac{1}{r}\frac{\partial u}{\partial r} + \frac{\partial^2 u}{\partial z^2} - \frac{u}{r^2}\right) \tag{6}$$

$$\frac{\partial w}{\partial t} + u\frac{\partial w}{\partial r} + w\frac{\partial w}{\partial z} = -\frac{1}{\rho}\frac{\partial p}{\partial z} + \nu\left(\frac{\partial^2 w}{\partial r^2} + \frac{1}{r}\frac{\partial w}{\partial r} + \frac{\partial^2 w}{\partial z^2}\right) \tag{7}$$

Thermal energy:

$$\frac{\partial T}{\partial t} + u\frac{\partial T}{\partial r} + w\frac{\partial T}{\partial z} = \alpha\left(\frac{\partial^2 T}{\partial r^2} + \frac{1}{r}\frac{\partial T}{\partial r} + \frac{\partial^2 T}{\partial z^2}\right) + \tau\left\{D_B\frac{\partial C}{\partial r}\frac{\partial T}{\partial r} + \frac{\partial C}{\partial z}\frac{\partial T}{\partial z} + \frac{D_T}{T_\infty}\left[\left(\frac{\partial T}{\partial r}\right)^2 + \left(\frac{\partial T}{\partial z}\right)^2\right]\right\}. \tag{8}$$

Nanoparticle volume fraction:

$$\frac{\partial C}{\partial t}+u\frac{\partial C}{\partial r}+w\frac{\partial C}{\partial z}=D_B\left(\frac{\partial^2 C}{\partial r^2}+\frac{1}{r}\frac{\partial C}{\partial r}+\frac{\partial^2 C}{\partial z^2}\right)+\frac{D_T}{T_\infty}\left(\frac{\partial^2 T}{\partial r^2}+\frac{1}{r}\frac{\partial T}{\partial r}+\frac{\partial^2 T}{\partial z^2}\right). \tag{9}$$

Due to axial symmetry, only two components in the cylindrical coordinates, i.e. r and z which are measured in the radial and axial directions, respectively (Fang et al. 2011).

The boundary conditions of these equations are taken to be

$$\begin{aligned}
&t<0: \quad u=w=0,\ T=T_\infty,\quad C=C_\infty \quad \text{for all} \quad r,z\\
&t\geq 0: \quad u=\frac{U}{\sqrt{1-\beta t}},\quad w=-\frac{1}{a_0^2}\frac{4\nu z}{1-\beta t},\quad T=T_w,\\
&\qquad\quad C=C_w \quad \text{at} \quad r=a(t)\\
&\qquad\quad w\to 0,\quad T\to T_\infty,\quad C\to C_\infty \quad \text{as} \quad r\to\infty,
\end{aligned} \tag{10}$$

where U (<0) is the constant mass transfer (suction) velocity; T_w is the constant surface temperature; C_w is the constant surface nanoparticle volume fraction; while T_∞ and C_∞ are the constant temperature and nanoparticle volume fraction far from the surface of the cylinder (inviscid fluid), respectively.

We now introduce the following similarity variables (Fang et al. 2012)

$$u=-\frac{1}{a_0}\frac{2\nu}{\sqrt{1-\beta t}}\frac{f(\eta)}{\sqrt{\eta}},\ w=\frac{1}{a_0^2}\frac{4\nu z}{1-\beta t}f'(\eta),$$

$$\theta=\frac{T-T_\infty}{T_w-T_\infty},\ \phi=\frac{C-C_\infty}{C_w-C_\infty},\quad \eta=\left(\frac{r}{a_0}\right)^2\frac{1}{1-\beta t}. \tag{11}$$

Based on the defined velocity components, it is clear to derive from (6) that the pressure gradient $\partial p/\partial r$ is a function of time t and r, which is independent on z. Mathematically, this can be written as $\partial p/\partial r = A(t, r)$ implies $p=\int A(t,r)\,dr+B(t,z)$ where $B(t, z)$ is the constant of the integration. Therefore, it can be shown that $\partial p/\partial z = \partial B(t, x)/\partial z$. Hence, $\partial p/\partial z$ is independent on r. Then, evaluating (7) at $r \to \infty$ yields $\partial p/\partial z = 0$ (Fang et al. 2012). Thus, substituting (11) into (7) to (9), we obtain the following ordinary differential equations (12)-(14) while (5) is satisfied automatically.

$$\eta f'''+f''+f f''-f'^2-S\left(\eta f''+f'\right)=0. \tag{12}$$

$$\frac{1}{\Pr}(\eta\theta''+\theta')+f\theta'-S\eta\theta'+\eta\,(Nb\phi'\theta'+Nt\theta'^2)=0. \tag{13}$$

$$\eta\phi''+\phi'+Le\,(f\phi'-S\eta\,\phi')+\frac{Nt}{Nb}(\eta\theta''+\theta')=0. \tag{14}$$

The boundary conditions (10) now become

$$\begin{aligned}
&f(1)=\gamma,\quad f'(1)=-1,\quad \theta(1)=1,\quad \phi(1)=1\\
&f'(\eta)\to 0,\quad \theta(\eta)\to 0,\quad \phi(\eta)\to 0 \quad \text{as} \quad \eta\to\infty,
\end{aligned} \tag{15}$$

where prime denotes differentiation with respect to η; Pr is the Prandtl number; Le is the Lewis number; γ is the suction parameter; S is the unsteadiness parameter; Nb is the Brownian motion parameter and Nt is the thermophoresis parameter, which are defined as

$$\Pr=\frac{\nu}{\alpha},\quad Le=\frac{\nu}{D_B},\quad \gamma=-\frac{a_0 U}{2\nu},\quad S=\frac{a_0^2\beta}{4\nu}$$

$$Nb=\frac{\tau D_B(C_w-C_\infty)}{\nu},\quad Nt=\frac{\tau D_T(T_w-T_\infty)}{\nu T_\infty}. \tag{16}$$

The suction parameter γ indicates the strength of the mass transfer at the surface, the constant S is the unsteadiness parameter for a contracting cylinder, displays the strength of the contraction. The Brownian motion parameter Nb can be observed as random drifting of suspended nanoparticles. The thermophoresis parameter Nt represents the nanoparticle migration due to imposed temperature gradient across the fluid.

Based on previous discussion, the fluid pressure does not depend on z. Therefore, the pressure can be obtained from (6) as,

$$\frac{p}{\rho}=const+\nu\left(\frac{\partial u}{\partial r}+\frac{u}{r}\right)-\frac{1}{2}u^2+\int\frac{\partial u}{\partial t}dr. \tag{17}$$

The quantities of physical interest are the skin friction coefficient C_f, the Nusselt number Nu_x and the Sherwood number Sh_x, which can be expressed as,

$$C_f=\frac{\tau_w}{\rho w_w^2/2},\quad Nu_x=\frac{a_0(1-\beta t)^{1/2}q_w}{2k(T_w-T_\infty)},\quad Sh_x=\frac{a_0(1-\beta t)^{1/2}q_m}{2D_B(C_w-C_\infty)}, \tag{18}$$

where τ_w is the surface shear stress; q_w is the surface heat flux; and q_m is the surface mass flux, which are defined as,

$$\tau_w=\mu\left(\frac{\partial w}{\partial r}\right)_{r=a(t)}=\frac{1}{a_0^3}\frac{8\nu\mu z}{(1-\beta t)^{3/2}}f''(1),$$

$$q_w=-k\left(\frac{\partial T}{\partial r}\right)_{r=a(t)}=\frac{2k(T_w-T_\infty)}{a_0(1-\beta t)^{1/2}}\left[-\theta'(1)\right],$$

$$q_m=-D_B\left(\frac{\partial C}{\partial r}\right)_{r=a(t)}=\frac{2D_B(C_w-C_\infty)}{a_0(1-\beta t)^{1/2}}\left[-\phi'(1)\right], \tag{19}$$

with μ being the dynamic viscosity; and k being the nanofluid thermal conductivity. Substituting (11) into (19), and using (18), we get

$$C_f z / a(t) = f''(1), \quad Nu_x = -\theta'(1), \quad Sh_x = -\phi'(1). \tag{20}$$

Results and Discussion

The system of nonlinear ordinary differential (12)-(14) subject to the boundary conditions (15) was solved numerically using a shooting method described by Jaluria and Torrance (2003). The numerical results are presented to carry out a parametric study showing the effects of the suction parameter γ and the unsteadiness parameter S on the velocity, temperature and concentration profiles as well as the heat transfer characteristics. In this method, dual solutions are obtained by using different initial guesses for the values of $f''(1), -\theta'(1)$ and $-\phi'(1)$, where all related profiles satisfy the far field boundary conditions (15) asymptotically but with different shapes and boundary layer thicknesses.

In order to show the validity and accuracy of the present numerical results obtained, we compare previously numerical results obtained with those of Fang et al. (2012, 2011) for the case of viscous flow without considering nanoparticles in the base fluid. Table 1 shows the comparison values of $f''(1)$ with those given by Fang et al. (2011) for the case of unsteady viscous flow over a stretching cylinder. This comparison was obtained by setting $f'(1) = 1$ (stretching case) in the boundary condition (15) and taking Re = 1 in (5) (Fang et al. 2011). The present numerical results has also been compared with those presented by Fang et al. (2012) for the unsteady viscous flow over an expanding or contracting cylinder by setting $f'(1) = 0$ in the boundary condition (15) as shown in Table 2. It can be observed that the comparisons are in excellent agreement, thus give confidence to the results for the shrinking cylinder case to be reported further. The values of the skin friction coefficient in terms of $f''(1)$, the Nusselt number $-\theta'(1)$ and the Sherwood number $-\phi'(1)$ which represent the friction, the heat transfer and the concentration rates at the surface respectively, are presented in Table 3 for several values of γ. It is seen that dual solutions exist for each particular values of γ. We term them first and second solutions with the first solution has larger value than the second solution.

Figures 2-4 show the variation of the skin friction coefficient, the Nusselt number and the Sherwood number as a function of S for some values of γ. For each values of S under the same values of γ, Le, Nt, Nb and Pr, there exist regions with dual solutions for $S < S_c$, unique solution for $S = S_c$ and no solution for $S > S_c$, as shown in Figures 2-4 where S_c is the critical value of S for which the solution exists. Table 4 presents the values of S_c for some values of γ. It is further observed that suction effect is to widen the range of S for which the solution exists, which clearly shown in Figures 2-4. It is worth to highlight that a stability analysis of the multiple solutions for similar flow problem has been done by Harris et al. (2009), Merkin (1985), Paullet and Weidman (2007), Postelnicu and Pop

TABLE 1. Comparison values of between Fang et al. (2011) and the present results for some values of S by setting in (15) and taking Re = 1 in (5) of Fang et al. (2011)

S	Fang et al. (2011)	Present result
0	-1.17775	-1.177759
-0.3		-1.297000
-0.5	-1.45646	-1.456464
-1	-2.01502	-2.015028
-1.2		-2.282471
-1.5		-2.718956
-2	-3.52458	-3.524662
-3		-5.372557
-5	-9.82401	-9.824007
-6		-12.372084
-7		-15.112519
-8		-18.033213
-9		-21.124250
-10		-24.377265
-12		-31.341307
-15		-42.847949
-18		-55.520620
-20		-64.569799

TABLE 2. Comparison values of $f''(1)$ between Fang et al. (2012) and present results for some values of S by setting $f'(1) = 0$ in (15)

S	Fang et al. (2012)	Present result
0	0	0
-0.3		-0.090281
-0.5	-0.1978	-0.197844
-1	-0.5791	-0.579146
-1.3		-0.870101
-1.5		-1.086412
-2	-1.6973	-1.697309
-3		-3.180683
-4.5		-5.952526
-5	-7.0031	-7.003505
-8		-14.444371
-9		-17.310887
-12		-26.919623
-15		-37.890590
-18		-50.079823
-20		-58.829355
-25		-82.706832
-30		-109.211140

TABLE 3. Values of $f''(1)$, $-\theta'(1)$, and $-\phi'(1)$ for different values of γ when $Le = 1$, $Nt = 0.5$, $Nt = 0.5$, $Nb = 0.5$, $\Pr = 6.2$ and $S = -1$

γ	$f''(1)$	$-\theta'(1)$	$-\phi'(1)$
1	1.00089 (0.07921)	4.64676 (4.83184)	-2.11997 (-2.45669)
1.5	1.91766 (-1.05283)	6.064570 (6.66062)	-3.068320 (-4.08398)
2	2.56321 (-2.15529)	7.51832 (8.37952)	-4.08006 (-5.50250)
3	3.70205 (-5.07561)	10.40620 (11.60719)	-6.06467 (-7.99609)
4	4.77219 (-9.29719)	13.254753 (14.65424)	-7.98109 (-10.2095)
5	5.81516 (-15.08764)	16.07301 (17.59806)	-9.84716 (-12.26569)
6	6.84433 (-22.65506)	18.87063 (20.48143)	-11.67947 (-14.23004)

( ) second solution

(2011), Rosca and Pop (2013) and Weidman et al. (2006). They showed that the first solutions are linearly stable and physically relevant, whereas the second solutions are not. We expect this finding hold to the present results.

In Figure 2, increasing values of γ is to increase the magnitude of $f''(1)$. Physically, this observation occurs because of the suction effect which increases the skin friction coefficient. In contrast, increasing S is to decrease the magnitude of $f''(1)$. In Figures 3 and 4, the increasing of γ increases both the heat transfer rate and the concentration rate (in absolute sense) at the surface. In contrast, it is seen that increasing S is to decrease (in absolute sense) both the heat transfer and the concentration rates at the surface, for both first and second solutions.

Figure 5 presents the effects of the suction parameter γ on the velocity profiles when the other parameters are fixed. For the first solution, which we expect to be the physically realizable solutions, it is seen that the velocity of the fluid inside the boundary layer decreases with increasing γ, as a consequence increases the velocity gradient at the

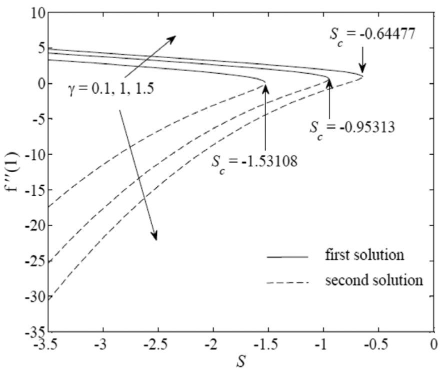

FIGURE 2. Variation of the skin friction coefficient with S for different values of γ when $Le = 1$, $Nt = 0.5$, $Nb = 0.5$ and $\Pr = 6.2$

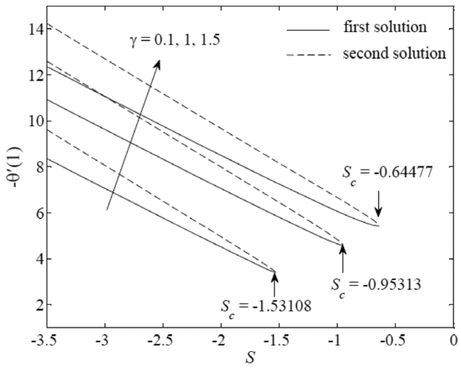

FIGURE 3. Variation of the Nusselt number with S for different values of γ when $Le = 1$, $Nt = 0.5$, $Nb = 0.5$ and $\Pr = 6.2$

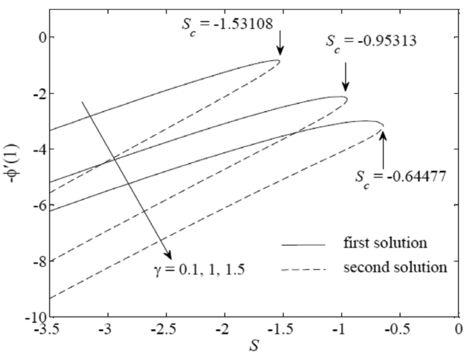

FIGURE 4. Variation of the Sherwood number with S for different values of γ when $Le = 1$, $Nt = 0.5$, $Nb = 0.5$ and $\Pr = 6.2$

surface. Therefore, the skin friction coefficient increases, which is consistent with the results presented in Figure 3. The opposite trend is observed for the second solution. It is further observed that the boundary layer thickness decreases with increasing γ for the first solution, due to the fact that the velocity penetration into the fluid becomes shorter in the presence of suction. It is also noticed that the positive velocity gradient at the surface is shown for the first solutions, while those of the second solutions have negative velocity gradient, which is again consistent with the results presented in Figure 2.

The suction effect on the temperature profiles is displayed in Figure 6. We found that the temperature decreases with increasing γ for both solutions. This observation occurs due to suction effect that decreases the thermal boundary layer thickness, which implies an increase in the temperature gradient at the surface. As a result, it increases the heat transfer rate at the surface as illustrated in Figure 3. The temperature difference between the first and second solutions is small compared to those of the velocity profiles presented in Figure 5.

Figure 7 is depicted to examine the influence of the suction parameter γ on the concentration profiles. It is noticed that concentration inside the boundary layer decreases as γ increases. All velocity, temperature and concentration profiles presented in Figures 5-7 satisfy the infinity boundary conditions (15) asymptotically, hence supporting the validity of the present numerical results, besides supporting the existence of the dual solutions shown in Figures 2-4.

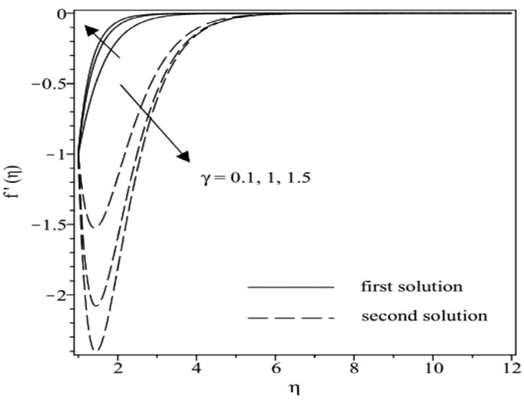

FIGURE 5. Effect of the suction parameter γ on the velocity profiles $f'(\eta)$ when $Le = 1$, $Nt = 0.5$, $Nb = 0.5$, $\Pr = 6.2$ and $S = -1$

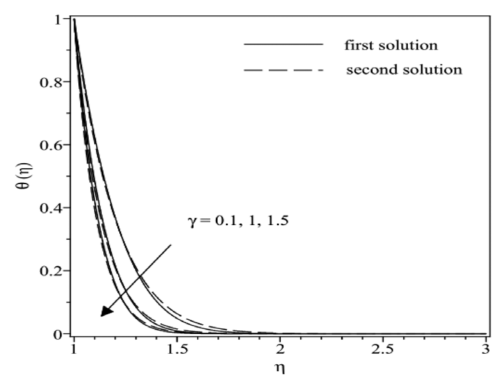

FIGURE 6. Effect of the suction parameter γ on the temperature profiles $\theta'(\eta)$ when $Le = 1$, $Nt = 0.5$, $Nb = 0.5$, $\Pr = 6.2$ and $S = -1$

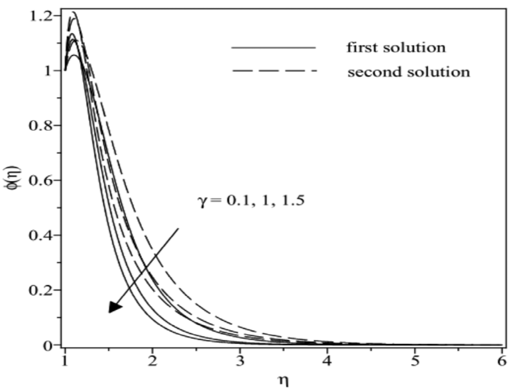

FIGURE 7. Effect of the suction parameter γ on the nanoparticle concentration profiles $\phi(\eta)$ when $Le = 1, Nt = 0.5, Nb = 0.5$, $\Pr = 6.2$ and $S = -1$

CONCLUSION

The problem of unsteady flow due to a permeable shrinking cylinder in a nanofluid using the nanofluid model proposed by Buongiorno was investigated. The transformed nonlinear ordinary differential equations were solved numerically using a shooting method. The effects of the suction and the unsteadiness parameters on the fluid flow and heat transfer characteristics were presented graphically and discussed. It is observed that suction increases the skin friction coefficient, the Nusselt number and the Sherwood number, in absolute sense. It was also found that increasing the unsteadiness parameter is to decrease the magnitude of the skin friction coefficient, the Nusselt number and the Sherwood number. Furthermore, it was found that non-unique solutions exist for a certain range of the suction and the unsteadiness parameters.

REFERENCES

Bejan, A. 2013. *Convection Heat Transfer.* 4th ed. New York: Wiley.

Buongiorno, J. 2006. Convective transport in nanofluids. *ASME Journal of Heat Transfer* 128: 240-250.

Choi, S.U.S. 1995. Enhancing thermal conductivity of fluids with nanoparticles. In *Developments and Application of Non-Newtonian Flows FED-vol. 231/MD* 66: 99-105.

Das, S.K., Choi, S.U.S., Yu, W. & Pradeep, T. 2007. *Nanofluids: Science and Technology.* New Jersey: Wiley-Interscience.

Dhanai, R., Rana, P. & Kumar, L. 2016. MHD mixed convection nanofluid flow and heat transfer over an inclined cylinder due to velocity and thermal slip effects: Buongiorno's model. *Powder Technology* 288: 140-150.

Duangthongsuk, W. & Wongwises, S. 2008. Effect of thermophysical properties models on the predicting of the convective heat transfer coefficient for low concentration nanofluid. *International Communications in Heat and Mass Transfer* 35: 1320-1326.

Fang, T., Zhang, J., Zhong, Y. & Tao, H. 2011. Unsteady viscous flow over an expanding stretching cylinder. *Chinese Physics Letters* 28. Article ID. 124707.

Fang, T., Zhang, J. & Zhong, Y. 2012. Note on unsteady viscous flow on the outside of an expanding or contracting cylinder. *Communications in Nonlinear Science and Numerical Simulation* 17: 3124-3128.

Harris, S.D., Ingham, D.B. & Pop, I. 2009. Mixed convection boundary layer flow near the stagnation point on a vertical surface in a porous medium: Brinkman model with slip. *Transport in Porous Media* 77: 267-285.

Ishak, A., Nazar, R. & Pop, I. 2008a. Uniform suction/blowing effect on flow and heat transfer due to a stretching cylinder. *Applied Mathematical Modelling* 32: 2059-2066.

Ishak, A., Nazar, R. & Pop, I. 2008b. Magnetohydrodynamic (MHD) flow and heat transfer due to a stretching cylinder. *Energy, Conversion and Management* 49: 3265-3269.

Kakac, S. & Pramuanjaroenkij, A. 2009. Review of convective heat transfer enhancement with nanofluids. *International Journal of Heat and Mass Transfer* 52: 3187-3196.

Jaluria, Y. & Torrance, K.E. 2003. *Computational Heat Transfer.* 2nd ed. New York: Taylor & Francis.

Kuznetsov, A.V. & Nield, D.A. 2010. Natural convective boundary-layer flow of a nanofluid past a vertical plate. *International Journal of Thermal Sciences* 49: 243-247.

Merkin, J.H. 1985. On dual solutions occurring in mixed convection in a porous medium. *Journal of Engineering Mathematics* 20: 171-179.

Mohamed, M.K.A., Noar, N.A.Z.M., Salleh, M.Z. & Ishak, A. 2016. Free convection boundary layer flow on a horizontal circular cylinder in a nanofluid with viscous dissipation. *Sains Malaysiana* 45(2): 289-296.

Mukhopadhyay, S. 2012. Mixed convection boundary layer flow along a stretching cylinder in porous medium. *Journal of Petroleum Science and Engineering* 96-97: 73-78.

Paullet, J. & Weidman, P.D. 2007. Analysis of stagnation point flow towards a stretching sheet. *International Journal of Nonlinear Mechanics* 42: 1084-1091.

Postelnicu, A. & Pop, I. 2011. Falkner-Skan boundary layer flow of a power-law fluid past a stretching wedge. *Applied Mathematics and Computation* 217: 4359-4368.

Rosca, A.V. & Pop, I. 2013. Flow and heat transfer over a vertical permeable stretching/shrinking sheet with a second order slip. *International Journal of Heat and Mass Transfer* 60: 355-364.

Simal, S., Rosselló, C., Berna, A. & Mulet, A. 1998. Drying of shrinking cylinder-shaped bodies. *Journal of Food Engineering* 37: 423-435.

Trisaksri, V. & Wongwises, S. 2007. Critical review of heat transfer characteristics of nanofluids. *Renewable, Sustainable Energy Review* 11: 512-523.

Wan Zaimi, W.M.K.A., Ishak, A. & Pop, I. 2013. Unsteady viscous flow over a shrinking cylinder. *Journal of the King Saud University-Science* 25: 143-148.

Wang, C.Y. 1988. Fluid flow due to a stretching cylinder. *Physics of Fluids* 31: 466-468.

Wang, C.Y. & Ng, C. 2011. Slip flow due to a stretching cylinder. *International Journal of Non-Linear Mechanics* 46: 1191-1194.

Wang, C.Y. 2012. Natural convection on a vertical stretching cylinder. *Communications in Nonlinear Science and Numerical Simulation* 17: 1098-1103.

Wang, X.Q. & Mujumdar, A.S. 2008. A review on nanofluids - Part I: Theoretical and numerical investigations. *Brazilian Journal of Chemical Engineering* 25: 613-630.

Weidman, P.D., Kubitschek, D.G. & Davis, A.M.J. 2006. The effect of transpiration on selfsimilar boundary layer flow over moving surfaces. *International Journal of Engineering Science* 44: 730-737.

Khairy Zaimi*
Institute of Engineering Mathematics
Universiti Malaysia Perlis
02600 Arau, Perlis Indera Kayangan
Malaysia

Anuar Mohd Ishak
Pusat Pengajian Sains Matematik
Fakulti Sains dan Teknologi
Universiti Kebangsaan Malaysia
43600 UKM Bangi, Selangor Darul Ehsan
Malaysia

Ioan Pop
Department of Mathematics
Babeş-Bolyai University
400084 Cluj-Napoca
Romania

*Corresponding author; email: khairy@unimap.edu.my

Received: 28 June 2016
Accepted: 18 April 2017